| Title | Study on decomposition process of NaAlH4 by in-situ TEM |
|---|---|
| Author(s) | Isobe, Shigehito; Yao, Hao; Wang, Yongming; Kawasaki, Hiroshi; Hashimoto, Naoyuki; Ohnuki, Somei |
| Citation | International Journal of Hydrogen Energy, 35(14), 7563-7567<br>https://doi.org/10.1016/j.ijhydene.2010.05.001 |
| Issue Date | 2010-07 |
| Doc URL | http://hdl.handle.net/2115/43792 |
| Type | article (author version) |
| File Information | IJHE35-14_7563-7567.pdf |

# Study on Decomposition Process of $NaAlH_4$ by In-situ TEM

Shigehito Isobe, Hao Yao, Yongming Wang, Hiroshi Kawasaki,

Naoyuki Hashimoto, Somei Ohnuki

*Graduate School of Engineering, Hokkaido University, Sapporo, Hokkaido, 060-8628, Japan*

Corresponding Author: isobe@eng.hokudai.ac.jp

Keywords: $NaAlH_4$, Hydrogen Storage, in-situ TEM, Glove Bag Method

**Abstract**

In-situ transmission electron microscopy (TEM) has been performed to observe decomposition process of sodium alanate ($NaAlH_4$) in this work. $NaAlH_4$ was ground in a glove box under inert gas, and then it was transferred into microscope without exposed to air by Plastic Bag Method. The results of in-situ electron beam diffraction showed that $NaAlH_4$ decomposed to $Na_3AlH_6$ + Al, and NaH + Al during heated up to 150, 200°C, respectively. Moreover, we obtained the result of high resolution (HR) TEM images about the decomposition of $NaAlH_4$ by high voltage electron microscopy (HVEM) of 1250 keV. It showed that the porous structures appeared with increase of temperature. This should be from structural defects and/or cavities due to volume change of the phases. It was also shown that $Na_3AlH_6$ and Al particles with the grain size of several ten nm were irregularly distributed near the pores.

## Introduction

Complex hydrides, such as $NaAlH_4$ and $LiBH_4$, are regarded as one of the promising candidates for hydrogen storage materials because of their high gravimetric hydrogen density [1]. Since the report by Bogdanovic and Schwickardi, which demonstrated the catalyst effect of Ti-dopants in the hydrogen absorption and desorption properties of $NaAlH_4$ [2], a lot of research works on $NaAlH_4$ have been reported all over the world. Hydrogen is released from $NaAlH_4$ via the following two reversible steps;

$$3NaAlH_4 \leftrightarrow Na_3AlH_6 + 2Al + 3H_2$$

$$Na_3AlH_6 \leftrightarrow 3NaH + Al + 3/2H_2.$$

$NaAlH_4$ has a total hydrogen capacity of 5.6 mass%, in which first and second reaction devotes 3.7 mass% and 1.9 mass%, respectively. In-situ X-ray powder diffraction was performed to understand the phase transition and the crystal structural change during the thermal decomposition of $NaAlH_4$ [7]. With respect to catalyst in $NaAlH_4$, some reports indicated that the Ti-dopants were reduced to the catalytically active zerovalent state of titanium during the doping process [3-5]. On the other hand, it can be assumed that the location of reaction events is at the phase boundary between Al particles and NaH, $Na_3AlH_6$ or $NaAlH_4$ phases [4, 6]. It was also suggested that some chemical association of Ti and Al probably existed after several absorption and desorption cycles [4, 8-11]. The microstructure of $NaAlH_4$ with $TiF_3$ additive has been investigated by using TEM, SEM and EDS, which showed there was no significant change in the grain size of Al after 15 cycles [10]. So far a lot of investigations on $NaAlH_4$ have been reported: nevertheless, the decomposition mechanism of $NaAlH_4$ and the role of Ti catalyst during the hydrogen absorption and desorption have not been completely clarified yet.

In this work, we observed the decomposition process of $NaAlH_4$ by in-situ high voltage electron beam microscope (HVEM) in order to understand the dehydrogenation mechanism. It is quite important to clarify the dehydrogenation mechanism of $NaAlH_4$ itself for understanding the catalysis mechanism of Ti-additives in $NaAlH_4$. High-resolution TEM (HRTEM) imaging, which is used as a unique technology to obtain micro-characterization in atomic level, is mostly utilized to be one of the best tools to analyze defects in materials. In addition, we carefully performed TEM observation, because $NaAlH_4$ is not stable to electron beam irradiation so much, and also performed several experimental methods such as "glove box" and "Plastic Bag Method" for obtaining trustworthy experimental data.

## Experimental

$NaAlH_4$ powder was purchased from Aldrich. In order to avoid the reactions between $NaAlH_4$ and $O_2$/$H_2O$ in air, all processes in preparing the samples were handled in the glove box filled with purified argon. $NaAlH_4$ powder was dispersed on Mo grid after ground for two minutes with an agate mortar by hand, and then the grid was set into the sample holder of HVEM. In-situ HVEM observation was performed by using JEM-ARM 1300 with accelerating voltage of 1250 kV at Hokkaido University in Japan. For transferring the sample holder from the glove box into HVEM, we set up Plastic Bag Method. In Plastic Bag Method, firstly the sample holder is sealed into a plastic bag under argon gas in the glove box, and then the holder is connected to HVEM. Before setting the holder into HVEM, the gas purge of the connected part with argon gas was carried out. By this method, we can minimize contamination from the reaction of sample and air. On the other hand, in order to minimize the knock-off damage and heat damage caused by the irradiation of electron beam in HVEM, the intensity of electron beam was limited during the observation. In-situ observation at the temperature range from R.T. to 200 °C was carried out by using the heating holder in HVEM. We obtained selected area electron beam diffraction (SAED) patterns and bright field (BF) images at R.T., 100 °C, 150 °C, and 200 °C. Especially at R.T., 150 °C, and 200 °C, HRTEM images were analyzed by using software Digital Micrograph (Gatan, Inc.).

## Results and Discussion

Figure 1 shows SAED patterns at R.T., 100 °C, 150 °C, and 200 °C. $NaAlH_4$ was identified in the patterns at R.T. and 100 °C. This indicates no decomposition occurs up to 100 °C. At 150 °C, the patterns were identified as $Na_3AlH_6$ and Al, which were the phases after proceeding of first reaction (1). NaH and Al, which were the phases after proceeding of second reaction (2), were identified at 200 °C. The phases identified at each temperature are summarized in Table 1. From the results of SAED, we confirmed the decomposition of $NaAlH_4$ occurred by in-situ HVEM. If we perform TEM experiment without Plastic Bag Method, sodium oxide and sodium hydroxide are observed in the results. It can be recognized that Plastic Bag Method is quite effective to avoid the reaction of $NaAlH_4$ and air.

$$3NaAlH_4 \rightarrow Na_3AlH_6 + 2Al + 3H_2 \qquad (1)$$

$$Na_3AlH_6 \rightarrow 3NaH + Al + 3/2H_2 \qquad (2)$$

Figure 2 shows BF images of the particle with diameter of around 200 nm at R.T., 100 °C, 150 °C, and 200 °C. There is almost no difference in the results at R.T. and 100 °C, which means that no reaction occurred up to 100 °C. These results are consistent with the results of SAED. In the images at 150 °C and 200 °C, several pores with diameter of around 10 nm were observed in the particle. Here, we can propose several possibilities to explain about the appearance of porous structure. One is due to volume change of the phases through two steps decomposition. The other is emission of hydrogen molecular, which might make some voids, and/or structural defects with increase of temperature. In Table 1, relative values of theoretical volume at each step are shown. Compared to “$NaAlH_4$” at R.T., the volume of “$Na_3AlH_6$ + Al” and “NaH + Al” becomes smaller. This indicates the particle should shrink or the density of the particle should become low. In the images, the particle size seems almost no change with the increase of temperature, that is, the density of particle become low. This would cause the appearance of pores. Therefore we are considering that the appearance of pores is due to volume change of the phases.

HRTEM images and FFT, IFFT images at R.T., 150 °C, and 200 °C are shown in Figure 3. In the HRTEM images, we found lattice images from several phases. For obviously recognizing the phases, we performed image analysis by Digital Micrograph. At R.T., all phases are identified as $NaAlH_4$, so this result is completely consistent to the SAED result as well. Because the result at 100 °C is same as that at R.T., we don’t show it here. At 150 °C, the phases of $Na_3AlH_6$ and Al were identified as shown in Figure 3 (b). The mean grain size of Al, which seems to be located in $Na_3AlH_6$ matrix, is several ten nm. This result shows that several Al grains are generated from one $NaAlH_4$ matrix during the first reaction (1) to $Na_3AlH_6$. It is indicated that not only H atoms but also Al atoms diffuse in the Na-Al-H matrix to form the phases of $Na_3AlH_6$ + Al with hydrogen desorption. At that time, Na atoms don’t move so much. Similar phenomenon occurred at 200 °C, as shown in Figure 3 (c). Several grains of Al, which size is ~20 nm, appeared in NaH matrix. During the second reaction (2), Al grain was not grown up, but the number of Al grain was increased.

Figure 4 shows a schematic during two steps dehydrogenation to explain the mechanism. Firstly, $NaAlH_4$ transforms into $Na_3AlH_6$ + Al with hydrogen desorption. In this process, Al atoms move from $NaAlH_4$ matrix to be several Al grains with the size of several ten nm, moreover, porous structure with the size of around 10 nm is locally formed due to the volume change. In second process, the number of Al grain is increased, in which the grain size of Al doesn’t change so much. Totally, it is indicated that Al and H atoms diffuse more than Na atoms in dehydrogenation process. This is first report on in-situ observation of decomposition of $NaAlH_4$ by HVEM. We obtained the microscopic information about dehydrogenation mechanism of $NaAlH_4$ itself. For understanding rehydrogenation mechanism and catalysis mechanism of Ti-dopant in $NaAlH_4$, further research works are necessary.

## Conclusion

In-situ TEM observation has been performed to clarify the decomposition processes of $NaAlH_4$. From SAED patterns, it was confirmed that the decomposition with two steps of $NaAlH_4$ occurred with increase of temperature. The dehydrogenation starting temperatures of the first reversible decomposition reactions is around 150 °C and it is elucidated that the second reaction finished at 200 °C. Several pores are observed with proceeding of the dehydrogenation reaction. We are considering that this appearance of pores is due to volume change of the phases. From HRTEM images, lattice images of $NaAlH_4$ at R.T., $Na_3AlH_6$ + Al at 150 °C, and NaH + Al at 200 were identified, then it is indicated that Al and H atoms diffuse more than Na atoms in dehydrogenation process. In addition, Plastic Bag Method was useful to minimize the pollution from air to the sample.

## References

[1] F. Schuth, B. Bogdanovic, M. Felderhoff, Light metal hydrides and complex hydrides for hydrogen storage, Chem. Comm. (2004) 2249-2258.

[2] B. Bogdanovic, M. Schwickardi, Ti-doped alkali metal aluminum hydrides as potential novel reversible hydrogen storage materials, J. Alloys. Compd. 253 (1997) 1-9.

[3] A. Leon, O. Kircher, J. Rothe, M. Fichtner, Chemical state and local structure around titanium atoms in $NaAlH_4$ doped with $TiCl_3$ using X-ray absorption spectroscopy, J. Phys. Chem.

B 108 (2004) 16372-16376.

[4] M. Felderhoff, K. Klementiev, W. Grunert, B. Spliethoff, B. Tesche, J. M. Bellosta von Colbe, B. Bogdanovic, M. Hartel, A. Pommerin, F. Schuth, C. Weidenthaler, Combined TEM-EDX and XAFS studies of Ti-doped sodium alanate., Phys. Chem. Chem. Phys. 6 (2004) 4369-4374.

[5] J. Graetz, J. J. Reilly, J. Johnson, A. Y. Ignatov, T. A. Tyson, X-ray absorption study of Ti-activated sodium aluminum hydride, Appl. Phys. Let. 85 (2004) 500-502.

[6] X. D. Kang, P. Wang, H. M. Cheng, Electron microscopy study of Ti-doped sodium aluminum hydride prepared by mechanical milling NaH/Al with Ti powder, J. Appl. Phys. 100 (2006) 034914-034914-6.

[7] K. J. Gross, S. Guthrie, S. Takara, G. Thomas, In-situ X-ray diffraction study of the decomposition of $NaAlH_4$, J. Alloys. Compd. 297 (2000) 270-281.

[8] D. D. Graham, L. F. Culnane, M. Sulic, C. M. Jensen, I. M. Robertson, Ti EELS standards for identification of catalytic species in $NaAlH_4$ hydrogen storage materials, J. Alloys. Compd. 446 (2007) 255-259.

[9] G. J. Thomas, K. J. Gross, N. Y. C. Yang, C. Jensen, Microstructural characterization of catalyzed $NaAlH_4$, J. Alloys. Compd. 330-332 (2002) 702-707.

[10] C. M. Andrei, J. C. Walmsley, H. W. Brinks, R. Holmestad, S. S. Srinivasan, C. M. Jensen, B. C. Hauback, Electron-microscopy studies of $NaAlH_4$ with $TiF_3$ additive: Hydrogen-cycling effects, Appl. Phys. A: Mater. Sci. Process. 80 (2005) 709-715.

[11] M. P. Pitt, P. E. Vullum, M. H. Sorby, M. P. Sulic, C. M. Jensen, J. C. Walmsley, R. Holmestad, B. C. Hauback, Structural properties of the nanoscopic $Al_{85}Ti_{15}$ solid solution observed in the hydrogen-cycled $NaAlH_4$+0.1$TiCl_3$ system, Acta Mat. 56 (2008) 4691-4701.

## Acknowledgement

This work has been partially supported by NEDO (Hydro Star). The authors gratefully acknowledge Mr. Kenji Sugawara for his support and help to use HVEM.

## Table and Figure captions

Table 1 Phases identified from SAED patterns in Figure 1, and theoretical volume of the phases

Figure 1 SAED patterns at R. T., 100 °C, 150 °C, and 200 °C

Figure 2 BF images at (i) R. T., (ii) 100 °C, (iii) 150 °C, and (iv) 200 °C

Figure 3 HRTEM, FFT and IFFT images at (a) R. T., (b) 150 °C, and (c) 200 °C

Figure 4 Schematic of decomposition process of $NaAlH_4$

Table 1

| Temperature | Identification | Volume |
|---|---|---|
| R. T. | $NaAlH_4$ | 100 |
| 150°C | $NaAlH_4$+$Na_3AlH_6$ + Al | 36 |
| 200°C | NaH + Al | 65 |

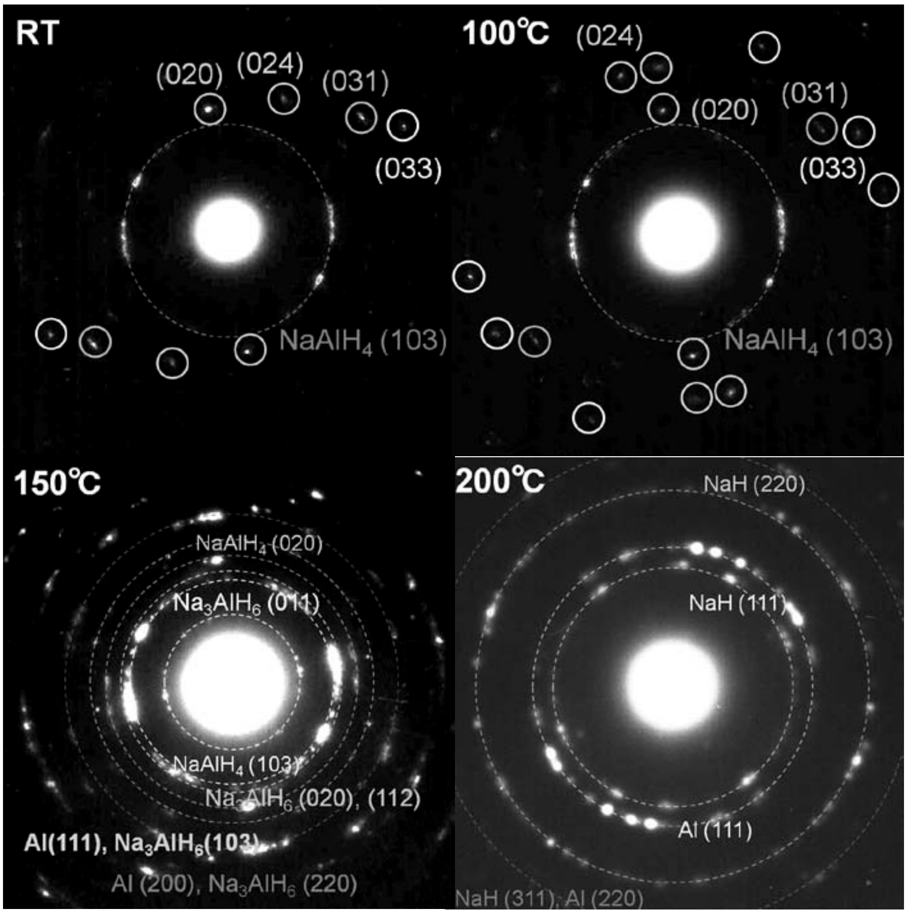
RT
(020)
(024)
(031)
(033)
NaAlH$_4$ (103)
100℃
(024)
(020)
(031)
(033)
NaAlH$_4$ (103)
150℃
NaAlH$_4$ (020)
Na$_3$AlH$_6$ (011)
NaAlH$_4$ (103)
Na$_3$AlH$_6$ (020), (112)
Al(111), Na$_3$AlH$_6$(103)
Al (200), Na$_3$AlH$_6$ (220)
200℃
NaH (220)
NaH (111)
Al (111)
NaH (311), Al (220)

Figure 1

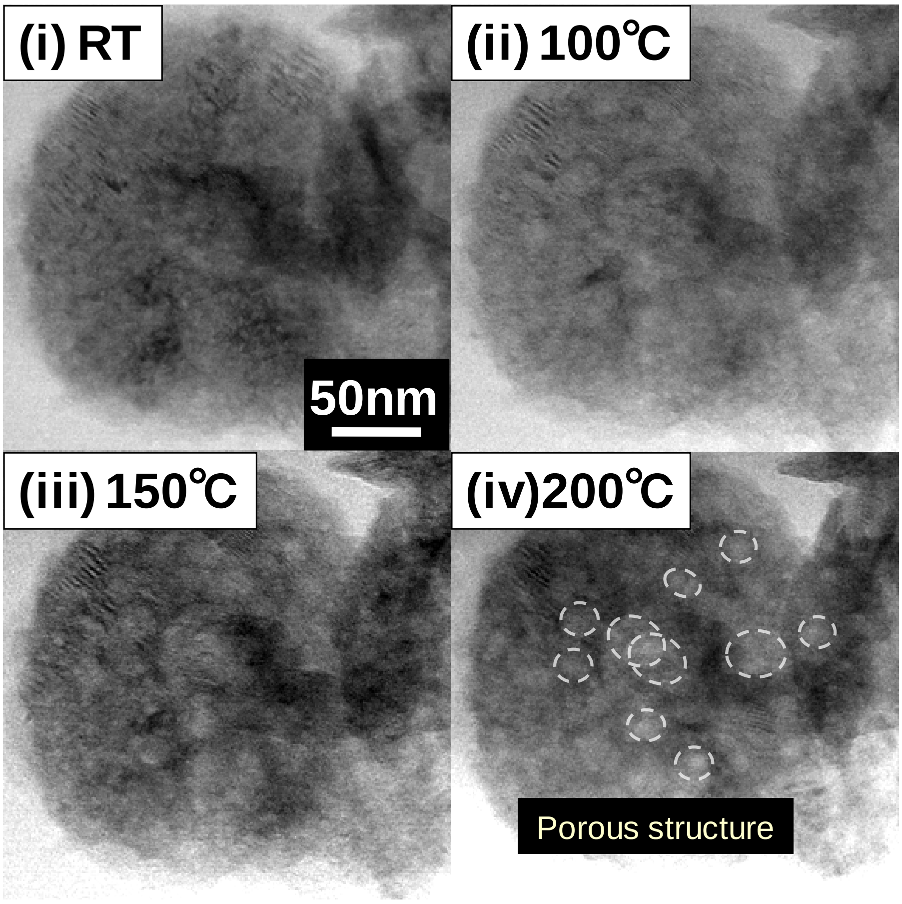


Figure 2

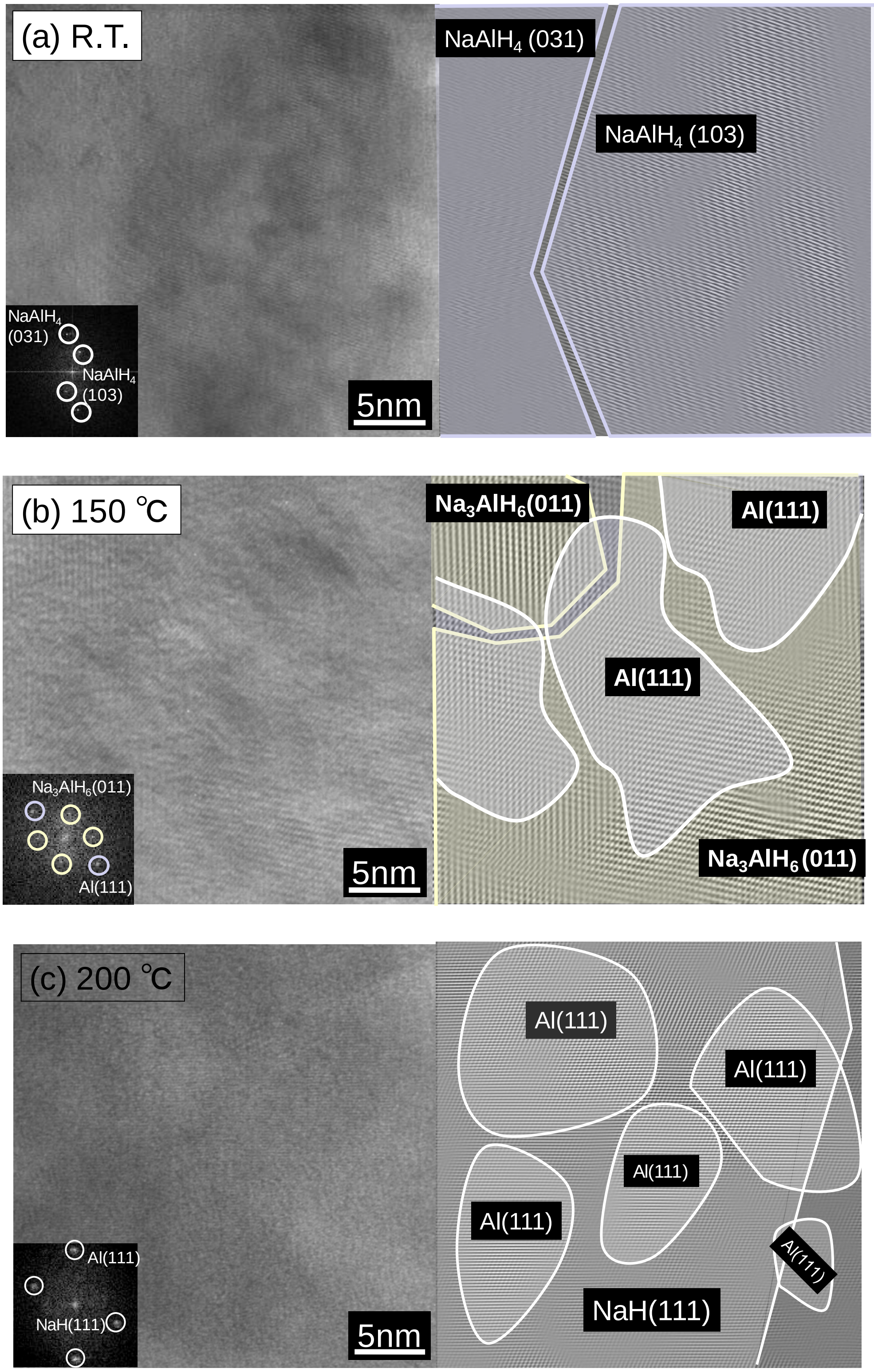

(a) R.T.
NaAlH4 (031)
NaAlH4 (103)
NaAlH4 (031)
NaAlH4 (103)
5nm
(b) 150 ℃
Na3AlH6(011)
Al(111)
Al(111)
Na3AlH6(011)
Na3AlH6(011)
Al(111)
5nm
(c) 200 ℃
Al(111)
Al(111)
Al(111)
Al(111)
Al(111)
NaH(111)
Al(111)
NaH(111)
5nm


Figure 3

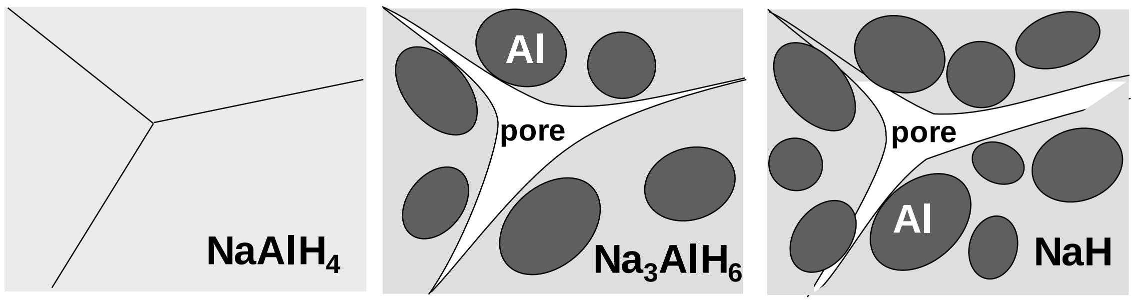


Figure 4